NASA Technical Memorandum 4384

Modified Optimal Control Pilot Model for Computer-Aided Design and Analysis

John B. Davidson
Langley Research Center
Hampton, Virginia

David K. Schmidt
Arizona State University
Tempe, Arizona

1. Summary

This paper presents the theoretical development of a modified optimal control pilot model based upon the optimal control model (OCM) of the human operator developed by Kleinman, Baron, and Levison (*Automatica,* May 1970). This model is input compatible with the OCM and retains other key aspects of the OCM, such as a linear quadratic solution for the pilot gains with inclusion of control rate in the cost function, a Kalman estimator, and the ability to account for attention allocation and perception threshold effects. Unlike the OCM, however, the structure of this model allows for direct calculation of pilot and system transfer functions in pole-zero form. An algorithm designed for easy implementation in current dynamic systems analysis and design software is presented. This implementation may be used for interactive modification of pilot-plant parameters, direct calculation of system and pilot transfer functions, system transfer function manipulation, and determination of system frequency responses. Example results based upon the analysis of a tracking task using three basic dynamic systems are compared with measured results and with similar analyses performed with the OCM and two previously proposed simplified optimal pilot models. The pilot frequency responses and error statistics obtained with this modified optimal control model are shown to compare more favorably with the measured results than the other previously proposed simplified models evaluated. Also, the impact on the modelling results of changing the approximation of the pilot's effective time delay is presented.

2. Introduction

Manual vehicular control system analysis, commonly referred to as pilot modelling, has been a useful tool for the analysis of pilot-in-the-loop systems. Research into the modelling of the pilot control behavior has its origins in studies of the human operator performed in the 1940's (Elkind 1964). From then until the 1960's, research was predominantly devoted to understanding the human as a controller of single-input/single-output systems using frequency domain models (McRuer 1980). Since the 1960's, research has concentrated on the analysis of more complex multivariate systems. Two basic approaches to analyzing these systems have emerged. One is based upon extending the frequency domain methods and insights developed for single-input/single-output systems to the multivariate case, and the other is based upon time domain methods and optimization theory (Innocenti 1988). This report focuses on a time domain approach.

The first attempt to describe the behavior of the human pilot in a time domain optimal control framework, the optimal control model (OCM), was by Kleinman, Baron, and Levison (Kleinman, Baron, and Levison 1970; Baron, Kleinman, and Levison 1970). The OCM is based upon the assumption that the well-trained and motivated human controller behaves optimally in some sense, adjusting the pilot's compensation for a given vehicle and task, subject to human limitations. The OCM has been widely used and has been validated in a number of tasks. It has been used to model task performance and to assess flying qualities, to model human-controller-describing functions, and for both the analysis and synthesis of manual control loops (Innocenti 1988). In the OCM, the pilot's compensation is modelled by linear-quadratic-regulator gains (Kwakernaak and Sivan 1972), a Kalman-Bucy filter (Kwakernaak and Sivan 1972), and a linear predictor (Kleinman, Baron, and Levison 1970).

This paper presents the theoretical development of a modified optimal control pilot model (MOCM) based upon the OCM of Kleinman, Baron, and Levison. This MOCM is a variation of simplified optimal pilot models developed by Hess (1976), Schmidt (1979 and 1981), and Broussard and Stengel (1977). This model is input compatible with the OCM and retains other key aspects of the OCM. Unlike the OCM, however, the structure allows for the direct calculation of pilot and system transfer functions in pole-zero form and is designed for easy implementation

in current dynamic systems analysis and design software. Thus, this implementation may also be used for interactive modification of pilot and plant parameters, system transfer function manipulation, and determination of system frequency responses.

Section 4 provides a theoretical development of the MOCM. In section 5, example results based upon the analysis of a tracking task using three basic dynamic systems are compared with measured experimental results (Kleinman, Baron, and Levison 1970) and similar analyses performed using the OCM and two previously proposed simplified optimal control pilot models (Hess 1976; Schmidt 1979).

3. Symbols

$\mathbf{A}$	system dynamic matrix
a_{th}	observation threshold
$\mathbf{B}$	system control matrix
$\mathbf{C}$	system output matrix
$\mathbf{D}$	system control to output matrix
$\mathbf{E}$	system disturbance matrix
E_{∞}	steady-state expected value
e	tracking error
erfc	error function
$\mathbf{F}$	Kalman filter gain matrix
f	cost function control-rate weighting
f_y	fraction of total attention
g_i	ith regulator gain
$\mathbf{g}_p$	regulator gain vector
H	pilot compensation transfer function
J_p	pilot objective function
$\mathbf{K}$	regulator Ricatti solution
k	transfer function gain
LQG	linear quadratic Gaussian
$\mathbf{l}_p$	pilot control gain vector
$\mathbf{l}_1$	augmented pilot control gain vector
MOCM	modified optimal control pilot model
n	vector dimension
OCM	optimal control model
$\mathbf{Q}_o$	augmented weighting matrix
$\mathbf{Q}_y$	cost function output weighting matrix
r	cost function control weighting
rms	root mean square

s	Laplace variable
t	time
u	control
$\mathbf{V}_u$	control noise intensity matrix
$\mathbf{V}_y$	observation noise intensity matrix
v_{dist}	velocity disturbance
$\mathbf{v}_p$	pilot disturbance
v_u	control noise disturbance
$\mathbf{v}_y$	observation noise disturbance
$\mathbf{W}$	state noise intensity matrix
$\mathbf{W}_1$	augmented noise intensity matrix
$\mathbf{w}$	state disturbance
$\mathbf{x}$	plant and disturbance state vector
$\mathbf{x}_d$	Pade delay state vector
x_{dist}	position disturbance
$\mathbf{y}$	pilot observation vector
δ	pilot input to plant
θ	system output
ρ	signal-to-noise ratio
$\mathbf{\Sigma}_1$	filter Ricatti solution matrix
σ	variance
τ	effective time delay
τ_η	"neuromotor" lag
χ	augmented state vector
Subscripts:	
c	pilot commanded control
d	delay
o	control-rate augmented system
obs	pilot observed
p	pilot
s	plant and delay augmented system
th	threshold
w	state disturbance
x	state
y	output
δ	pilot-plant input
1	plant and pilot augmented system

Superscripts:

T transpose

-1 inverse

$*$ optimal

A dot over a symbol denotes a derivative with respect to time; a carat over a symbol denotes an estimate.

4. Theoretical Development

This section presents a theoretical development of the modified optimal control pilot model (MOCM). A block diagram of the model components of the MOCM is given in figure 1. The notation has been chosen to be compatible with the OCM development (Kleinman, Baron, and Levison 1970). To simplify the notation, this development considers the case of a single control input, although the algorithm can easily be extended to account for multiple inputs.

The plant dynamics to be controlled, augmented with plant disturbance dynamics, are given by the state space time invariant linear equations:

$$\left.\begin{array}{c} \dot{\mathbf{x}} = \mathbf{Ax} + \mathbf{B}\delta + \mathbf{Ew} \\ \mathbf{y} = \mathbf{Cx} + \mathbf{D}\delta \end{array}\right\} \tag{4.1}$$

where $\mathbf{x}(t)$ is an n_x-dimensional state vector composed of both plant and system disturbance states, $\delta(t)$ is a scalar plant input, $\mathbf{w}(t)$ is an n_w-dimensional disturbance vector modelled as a zero mean Gaussian white noise process with intensity $\mathbf{W}$, and $\mathbf{y}(t)$ is an n_y-dimensional output vector.

The vector $\mathbf{y}_{\mathrm{obs}}(t)$, of dimension n_y, represents variables the pilot can perceive, either by observation or feel. The outputs observed by the pilot are assumed to be corrupted by an observation noise, $\mathbf{v}_y(t)$, a zero mean Gaussian white noise process with intensity $\mathbf{V}_y$:

$$\mathbf{y}_{\mathrm{obs}} = \mathbf{Cx} + \mathbf{D}\delta + \mathbf{v}_y$$

In the MOCM, the pilot's effective time delay is modelled by a Pade approximation. The pilot's effective time delay is placed at each of the pilot's outputs and is treated as part of the plant dynamics for determination of the pilot's regulation and filter gains. Since typically the
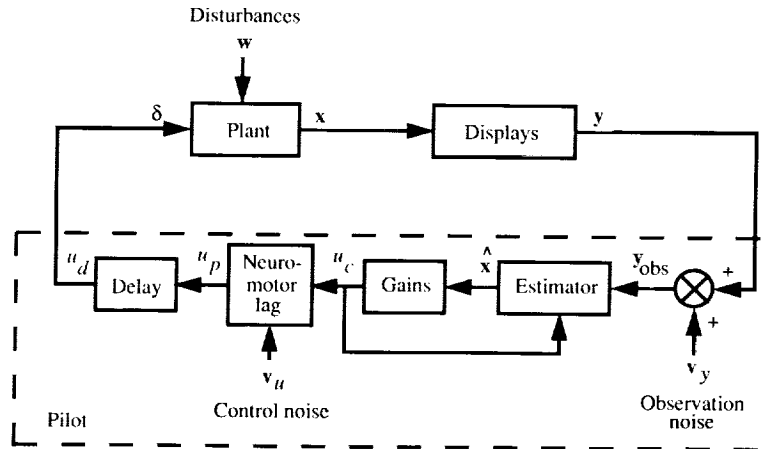

Figure 1. Conceptual block diagram of modified optimal control model.

4

pilot is modelled as having more inputs (observations) than outputs (plant inputs), placing the effective time delay at his output yields a lower order representation than placing the delay at his input. A second-order Pade approximation is chosen because it provides a very good approximation to a pure delay over the pilot's frequency range of interest (approximately 0.1 to 10 rad/sec). Use of at least a second-order Pade approximation is assumed to be necessary to accurately model pilot magnitude and phase compensation at the high end of the pilot's bandwidth, such as the pilot high frequency neuromotor resonant peak. Accurate representations of the pilot's resonant peak and phase compensation near crossover are necessary when concerned with using the model to explore pilot-vehicle dynamic interactions or predict pilot workload in a given task (Anderson and Schmidt 1987; Bacon and Schmidt 1983).

A second-order Pade approximation is given by

$$\frac{u_d}{u_p} = \frac{1 - \frac{1}{2}(\tau s) + \frac{1}{8}(\tau s)^2}{1 + \frac{1}{2}(\tau s) + \frac{1}{8}(\tau s)^2} \tag{4.2}$$

where τ is the delay interval (in seconds), u_p is the pilot's output, and u_d is the delayed pilot's output. In state space form, this can be expressed by

$$\left.\begin{aligned} \dot{\mathbf{x}}_d &= \mathbf{A}_d \mathbf{x}_d + \mathbf{B}_d u_p \\ \delta &= u_d = \mathbf{C}_d \mathbf{x}_d + u_p \end{aligned}\right\} \tag{4.3}$$

where $\mathbf{x}_d$ is a two-element vector of Pade delay states.

The plant dynamics augmented with the pilot's effective time delay are given by

$$\left.\begin{aligned} \frac{d}{dt}\left\{\begin{array}{c} \mathbf{x} \\ \mathbf{x}_d \end{array}\right\} &= \left[\begin{array}{cc} \mathbf{A} & \mathbf{B}\mathbf{C}_d \\ 0 & \mathbf{A}_d \end{array}\right]\left\{\begin{array}{c} \mathbf{x} \\ \mathbf{x}_d \end{array}\right\} + \left[\begin{array}{c} \mathbf{B} \\ \mathbf{B}_d \end{array}\right]u_p + \left[\begin{array}{c} \mathbf{E} \\ 0 \end{array}\right]\mathbf{w} \\ \mathbf{y} &= [\begin{array}{cc} \mathbf{C} & \mathbf{D}\mathbf{C}_d \end{array}]\left\{\begin{array}{c} \mathbf{x} \\ \mathbf{x}_d \end{array}\right\} + \mathbf{D}u_p \end{aligned}\right\} \tag{4.4a}$$

or

$$\left.\begin{aligned} \dot{\mathbf{x}}_s &= \mathbf{A}_s \mathbf{x}_s + \mathbf{B}_s u_p + \mathbf{E}_s \mathbf{w} \\ \mathbf{y} &= \mathbf{C}_s \mathbf{x}_s + \mathbf{D}_s u_p \end{aligned}\right\} \tag{4.4b}$$

The pilot's observation vector is given by

$$\mathbf{y}_{\text{obs}} = \mathbf{C}_s \mathbf{x}_s + \mathbf{D}_s u_p + \mathbf{v}_y$$

This model makes the assumption that the pilot's control task can be defined by the minimization of the quadratic performance index J_p given by

$$J_p = E_\infty \left\{ \mathbf{y}^T \mathbf{Q}_y \mathbf{y} + u_p^2 r + \dot{u}_p^2 f \right\} \tag{4.5}$$

subject to pilot observations $\mathbf{y}_{\text{obs}}$ with cost functional weightings $\mathbf{Q}_y \geq 0$, $r \geq 0$, and $f > 0$. By defining a new state vector as

$$\chi^T = [\begin{array}{cc} \mathbf{x}_s & u_p \end{array}]^T$$

the system given by equations (4.4) can be expressed in a control-rate formulation (Kwakernaak and Sivan 1972) as

$$\frac{d}{dt}\left\{\begin{array}{c} \mathbf{x} \\ \mathbf{x}_d \\ u_p \end{array}\right\} = \begin{bmatrix} \mathbf{A} & \mathbf{BC}_d & \mathbf{B} \\ \mathbf{0} & \mathbf{A}_d & \mathbf{B}_d \\ \mathbf{0} & \mathbf{0} & \mathbf{0} \end{bmatrix} \left\{\begin{array}{c} \mathbf{x} \\ \mathbf{x}_d \\ u_p \end{array}\right\} + \begin{bmatrix} 0 \\ 0 \\ 1 \end{bmatrix} \dot{u}_p + \begin{bmatrix} \mathbf{E} \\ 0 \\ 0 \end{bmatrix} \mathbf{w} \left.\begin{array}{c} \\ \\ \\ \\ \\ \\ \\ \\ \end{array}\right\}$$

$$\mathbf{y}_{\mathrm{obs}} = [\,\mathbf{C} \quad \mathbf{DC}_d \quad \mathbf{D}\,]\left\{\begin{array}{c} \mathbf{x} \\ \mathbf{x}_d \\ u_p \end{array}\right\} + \mathbf{v}_y \qquad \qquad (4.6a)$$

or

$$\left.\begin{array}{c} \dot{\chi} = \mathbf{A}_o\chi + \mathbf{B}_o\dot{u}_p + \mathbf{E}_o\mathbf{w} \\ \mathbf{y}_{\mathrm{obs}} = \mathbf{C}_o\chi + \mathbf{v}_y \end{array}\right\} \qquad \qquad (4.6b)$$

The minimizing control law is obtained by application of LQG solution techniques (Kwakernaak and Sivan 1972) to the augmented system (eqs. (4.6)); this leads to the full-state feedback relation

$$\dot{u}_p^* = -\mathbf{g}_p\widehat{\chi} = -\,[g_1, \ \ldots, \ g_n, \ g_{n+1}]\,\widehat{\chi} = -f^{-1}\,(\mathbf{B}_o)^T\,\mathbf{K}\widehat{\chi} \qquad \qquad (4.7)$$

where $n = n_x + 2$ (system states plus two Pade states), $\widehat{\chi}$ is the estimate of the state χ, and $\mathbf{K}$ is the unique positive definite matrix solution of the Ricatti equation

$$0 = (\mathbf{A}_o)^T\,\mathbf{K} + \mathbf{K}\mathbf{A}_o + \mathbf{Q}_o - \mathbf{K}\mathbf{B}_o f^{-1}\,(\mathbf{B}_o)^T\,\mathbf{K} \qquad \qquad (4.8)$$

where

$$\mathbf{Q}_o = \begin{bmatrix} (\mathbf{C}_s)^T\,\mathbf{Q}_y\mathbf{C}_s & (\mathbf{C}_s)^T\,\mathbf{Q}_y\mathbf{D}_s \\ (\mathbf{D}_s)^T\,\mathbf{Q}_y\mathbf{C}_s & (\mathbf{D}_s)^T\,\mathbf{Q}_y\mathbf{D}_s + r \end{bmatrix}$$

By expanding the optimal control law (eq. (4.7)) in terms of $\hat{\mathbf{x}}_s$ and u_p^*

$$\dot{u}_p^* = -\,[g_1, \ \ldots, \ g_n]\,\hat{\mathbf{x}}_s - g_{n+1}u_p^* \qquad \qquad (4.9)$$

and letting

$$\tau_\eta = \frac{1}{g_{n+1}}$$

and

$$\mathbf{l}_p = \tau_\eta\,[g_1, \ \ldots, \ g_n]$$

one obtains

$$\tau_\eta\dot{u}_p^* + u_p^* = u_c \qquad \qquad (4.10)$$

where the pilot's commanded control u_c is given by

$$u_c = -\mathbf{l}_p\hat{\mathbf{x}}_s \qquad \qquad (4.11)$$

To account for the uncertainty of the human operator's control input, control noise v_u is added to the commanded control u_c:

$$\tau_\eta\dot{u}_p + u_p = u_c + v_u \qquad \qquad (4.12)$$

where $v_u(t)$ is a zero mean Gaussian white noise process with intensity $\mathbf{V}_u$. As in the OCM development, the controller gains are assumed not to be affected by the inclusion of the control

6

noise (Kleinman, Baron, and Levison 1970). This assumption reduces the solution of the MOCM to a suboptimal control law. Solving for $\dot{u}_p$, one obtains

$$\dot{u}_p = \frac{-1}{\tau_\eta} u_p + \frac{1}{\tau_\eta} u_c + \frac{1}{\tau_\eta} v_u \tag{4.13}$$

Combining equations (4.6) and (4.13) gives

$$\left. \begin{aligned}
\frac{d}{dt} \left\{ \begin{array}{c} \mathbf{x} \\ \mathbf{x}_d \\ u_p \end{array} \right\} &= \begin{bmatrix} \mathbf{A} & \mathbf{BC}_d & \mathbf{B} \\ 0 & \mathbf{A}_d & \mathbf{B}_d \\ 0 & 0 & -1/\tau_\eta \end{bmatrix} \left\{ \begin{array}{c} \mathbf{x} \\ \mathbf{x}_d \\ u_p \end{array} \right\} + \begin{bmatrix} 0 \\ 0 \\ 1/\tau_\eta \end{bmatrix} u_c + \begin{bmatrix} \mathbf{E} & 0 \\ 0 & 0 \\ 0 & 1/\tau_\eta \end{bmatrix} \left\{ \begin{array}{c} \mathbf{w} \\ v_u \end{array} \right\} \\
\mathbf{y}_{\text{obs}} &= \begin{bmatrix} \mathbf{C} & \mathbf{DC}_d & \mathbf{D} \end{bmatrix} \left\{ \begin{array}{c} \mathbf{x} \\ \mathbf{x}_d \\ u_p \end{array} \right\} + \mathbf{v}_y
\end{aligned} \right\} \tag{4.14a}$$

or

$$\left. \begin{aligned}
\dot{\chi} &= \mathbf{A}_1 \chi + \mathbf{B}_1 u_c + \mathbf{E}_1 \mathbf{w}_1 \\
\mathbf{y}_{\text{obs}} &= \mathbf{C}_1 \chi + \mathbf{v}_y
\end{aligned} \right\} \tag{4.14b}$$

The current estimate of the state $\widehat{\chi}$ is given by a Kalman filter

$$\left. \begin{aligned}
\dot{\widehat{\chi}} &= \mathbf{A}_1 \widehat{\chi} + \mathbf{B}_1 u_c + \mathbf{F}\left(\mathbf{y}_{\text{obs}} - \hat{y}\right) \\
\dot{\widehat{\chi}} &= \left(\mathbf{A}_1 - \mathbf{FC}_1\right) \widehat{\chi} + \mathbf{FC}_1 \chi + \mathbf{B}_1 u_c + \mathbf{Fv}_y
\end{aligned} \right\} \tag{4.15}$$

where

$$\mathbf{F} = \Sigma_1 \left(\mathbf{C}_1\right)^T \left(\mathbf{V}_y\right)^{-1}$$

The covariance matrix of the estimation error Σ_1 is the unique positive definite solution of the Ricatti equation:

$$0 = \mathbf{A}_1 \Sigma_1 + \Sigma_1 \left(\mathbf{A}_1\right)^T + \mathbf{W}_1 - \Sigma_1 \left(\mathbf{C}_1\right)^T \left(\mathbf{V}_y\right)^{-1} \mathbf{C}_1 \Sigma_1 \tag{4.16}$$

where $\mathbf{W}_1 = \text{diag}(\mathbf{W}, \mathbf{V}_u)$ with $\mathbf{W} \geq 0, \mathbf{V}_u \geq 0$, and $\mathbf{V}_y > 0$.

A state space representation of the closed-loop pilot-vehicle system is given by

$$\left. \begin{aligned}
\frac{d}{dt} \left\{ \begin{array}{c} \chi \\ \widehat{\chi} \end{array} \right\} &= \begin{bmatrix} \mathbf{A}_1 & -\mathbf{B}_1 \mathbf{l}_1 \\ \mathbf{FC}_1 & \mathbf{A}_1 - \mathbf{B}_1 \mathbf{l}_1 - \mathbf{FC}_1 \end{bmatrix} \left\{ \begin{array}{c} \chi \\ \widehat{\chi} \end{array} \right\} + \begin{bmatrix} \mathbf{E}_1 & 0 \\ 0 & \mathbf{F} \end{bmatrix} \left\{ \begin{array}{c} \mathbf{w}_1 \\ \mathbf{v}_y \end{array} \right\} \\
\left\{ \begin{array}{c} \mathbf{y}_{\text{obs}} \\ \delta \end{array} \right\} &= \begin{bmatrix} \mathbf{C}_1 & 0 \\ \mathbf{C}_\delta & 0 \end{bmatrix} \left\{ \begin{array}{c} \chi \\ \widehat{\chi} \end{array} \right\}
\end{aligned} \right\} \tag{4.17}$$

where $\mathbf{l}_1 = \begin{bmatrix} \mathbf{l}_p & 0 \end{bmatrix}$ and $\mathbf{C}_\delta = \begin{bmatrix} 0 & \mathbf{C}_d & 1 \end{bmatrix}$.

A block diagram of the model components of the pilot's dynamics is given in figure 2. A state space representation of the pilot's dynamics is given by

$$\left. \begin{aligned}
\frac{d}{dt} \left\{ \begin{array}{c} \widehat{\chi} \\ u_p \\ \mathbf{x}_d \end{array} \right\} &= \begin{bmatrix} \mathbf{A}_1 - \mathbf{FC}_1 - \mathbf{B}_1 \mathbf{l}_1 & 0 & 0 \\ \mathbf{l}_1/\tau_\eta & -1/\tau_\eta & 0 \\ 0 & \mathbf{B}_d & \mathbf{A}_d \end{bmatrix} \left\{ \begin{array}{c} \widehat{\chi} \\ u_p \\ \mathbf{x}_d \end{array} \right\} + \begin{bmatrix} \mathbf{F} \\ 0 \\ 0 \end{bmatrix} y + \begin{bmatrix} \mathbf{F} & 0 \\ 0 & 1/\tau_\eta \\ 0 & 0 \end{bmatrix} \left\{ \begin{array}{c} \mathbf{v}_y \\ v_u \end{array} \right\} \\
\delta &= \begin{bmatrix} 0 & 1 & \mathbf{C}_d \end{bmatrix} \left\{ \begin{array}{c} \widehat{\chi} \\ u_p \\ \mathbf{x}_d \end{array} \right\}
\end{aligned} \right\} \tag{4.18a}$$

or

$$\left.\begin{array}{l} \dot{\mathbf{x}}_p = \mathbf{A}_p\mathbf{x}_p + \mathbf{B}_p\mathbf{y} + \mathbf{E}_p\mathbf{v}_p \\ \delta = \mathbf{C}_p\mathbf{x}_p \end{array}\right\} \qquad (4.18b)$$
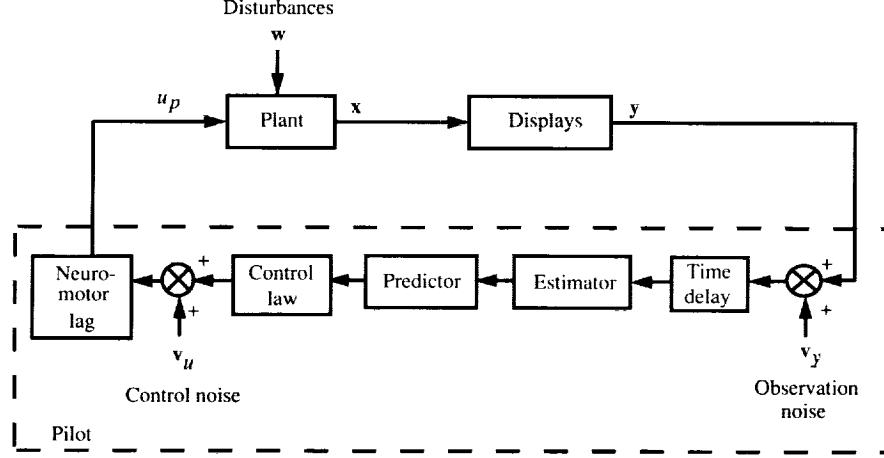

Figure 2. Conceptual block diagram of optimal control model.

4.1. OCM Overview

For reference, a brief description of the OCM is presented. A conceptual block diagram of the OCM is given in figure 2. For a more detailed description the reader is referred to Kleinman, Baron, and Levison 1970. The OCM of the pilot is based on the assumption that the pilot chooses the control input in such a way as to minimize the quadratic cost function:

$$J_{\text{OCM}} = E_\infty \left\{ \mathbf{y}^T \mathbf{Q}_y \mathbf{y} + u_p^2 r + \dot{u}_p^2 f \right\}$$

The weighting matrices in the cost function are chosen to reflect the task objectives and pilot physiological limitations. The human perception characteristics that are modelled involve pilot observations passed through a pure time delay and corrupted by white noise $\mathbf{v}_y$:

$$\mathbf{y}_{\text{obs}}(t) = \mathbf{y}(t - \tau) + \mathbf{v}_y(t - \tau)$$

The solution to this optimization problem yields a Kalman filter to estimate the delayed states and a least-mean-squares predictor to obtain a current estimate of the states $\hat{\mathbf{x}}$. The control law, obtained from minimizing the cost function J_{OCM} for a scalar control input u_p is given by

$$\tau_\eta \dot{u}_p + u_p = u_c(t) + v_u(t)$$

$$u_c(t) = -\mathbf{K}_{\text{OCM}} \, \hat{\mathbf{x}}(t)$$

where $\mathbf{K}_{\text{OCM}}$ is the optimal pilot control gain vector and τ_η is the pilot neuromotor lag obtained by including control rate in the cost function.

The MOCM is based on the same premise as the OCM- the assumption that the well-trained and motivated human controller adjusts his compensation, subject to human limitations, for a given vehicle and task to minimize an objective function. Similarities to the OCM structure include a linear quadratic solution for the pilot gains with inclusion of control rate in the cost function, a Kalman estimator, and the ability to account for attention allocation and perception threshold effects. The major difference between the OCM and the MOCM is the replacement of

8

the linear predictor of the OCM by the augmentation of the system dynamics with the pilot's effective time delay before calculation of pilot control and estimation gains. This difference allows for the direct calculation of the pilot and system transfer functions in pole-zero form in the MOCM.

4.2. MOCM Pilot Parameters

The pilot cost function weighting matrices $\mathbf{Q}$ and r are chosen to reflect the pilot task objective. Values for effective time delay, neuromotor lag, observation, and control noise intensities are chosen in the same manner as for the OCM (Kleinman, Baron, and Levison 1970). Appropriate values of neuromotor lag τ_η are obtained by appropriate choice of pilot cost function control-rate weighting f. Manual control experiments have shown that the effective time delay of the pilot τ is typically 0.1 to 0.2 second (Kleinman, Baron, and Levison 1970).

The covariance of the observation noise $\mathbf{V}_y$ is dependent upon the nature of the display, human limitations, and the pilot's environment. Over a wide range of viewing conditions, each diagonal element of the observation noise intensity matrix is proportional to the variance of its associated observed output variable. The diagonal elements of the noise intensity matrix are given by

$$\mathbf{V}_{y_i} = \frac{\pi \rho_{y_i}}{f_{y_i}} \frac{\sigma_{y_i}^2}{\mathrm{erfc}\left(a_{\mathrm{th}_i}/\sigma_{y_i}\sqrt{2}\right)} \qquad (i = 1, 2, \ldots, n_y) \qquad (4.19)$$

where ρ_{y_i} is the nominal full-attention observation signal-to-noise ratio, f_{y_i} is the fraction of total attention spent on the ith observation variable, a_{th_i} is the minimum observation threshold of the ith observation variable, and $\sigma_{y_i}^2$ is the variance of the ith observation. Single-axis manual tracking control tasks have shown that, on the average, $\rho_{y_i} = 0.01$, which corresponds to a normalized observation noise of -20 dB (Kleinman, Baron, and Levison 1970).

The covariance of the control noise $\mathbf{V}_u$ is assumed to be proportional to the variance of the commanded control u_c:

$$\mathbf{V}_{u_i} = \pi \rho_{u_i} \sigma_{u_i}^2 \qquad (i = 1, 2, \ldots, n_u) \qquad (4.20)$$

where ρ_u is the control signal-to-noise ratio. Analyses of single-axis manual tracking control task experiments have shown that typically $\rho_{u_i} = 0.003$, which corresponds to a normalized control noise ratio of -25 dB (Kleinman, Baron, and Levison 1970).

4.3. MOCM Algorithm Implementation

The MOCM algorithm is organized into four major parts. The first part involves augmentation of the plant and disturbance dynamics with a Pade approximation of the pilot's effective time delay. The second part is the calculation of the pilot's control gains, where iteration on the cost function control-rate weighting is usually required to achieve the desired value of pilot's neuromotor time constant. The third part is the calculation of the pilot's estimation gains. This requires the calculation of observation and control noise covariances to yield desired signal-to-noise ratios for the pilot model. At this step, the observation noise covariance may be adjusted to take into account pilot scanning behavior and observation threshold effects. The fourth part involves formation of pilot and closed-loop system matrices and calculation of transfer functions, frequency responses, and statistics of interest. A conceptual flowchart of the MOCM algorithm is given as appendix A.

The structure of this model is designed for easy implementation in current dynamic systems analysis and design software. Implementation in this type of computer software environment

allows for rapid calculation of pilot and system transfer function descriptions from state space models, determination of system frequency responses, and easy manipulation of system state space and frequency domain representations. Also, this environment allows users to interactively modify various pilot and plant parameters and quickly ascertain the impact of these changes on pilot/closed-loop performance.

Section 5 presents an evaluation of the MOCM by applying it to model the piloted dynamics of a compensatory tracking task.

5. Model Evaluation

In this section, experimental results based upon the analysis of the closed-loop performance of a pilot in a tracking task for three basic dynamic systems presented in Kleinman, Baron, and Levison 1970 are used as a benchmark to determine the merits of the MOCM. The analysis obtained with this model is compared with similar analyses performed with the OCM and two previously proposed LQG based pilot models—an LQG approximation to the OCM presented by Schmidt (LQG model) (Schmidt 1979), and a pilot model proposed by Hess (Hess model) (Hess 1976). The LQG model includes a control-rate term in the pilot cost function and a Kalman estimator but does not include an explicit model of the pilot's effective time delay. The Hess model does not include a control-rate term in the pilot's cost function but does include a Kalman estimator and a modelling of the pilot's effective time delay. In this model, the pilot's neuromotor dynamics are modelled by a first-order lag at the pilot's output. A description of these models is given in appendixes B and C. Also, the impact of changing the order of the Pade approximation (approximation of pilot's effective time delay) upon the MOCM results is presented.

Descriptions of the three basic dynamic systems, the tracking task, and parameters chosen for the modelling analysis are presented next. This discussion parallels that in Kleinman, Baron, and Levison 1970.

5.1. Experimental Setup

The compensatory tracking task performed and analyzed by Kleinman, Baron, and Levison used three basic command systems—a velocity command system, an acceleration command system, and a position command system. In these experiments, the human controller had a single control manipulator and observed tracking error on a display. The assumption was made that the pilot could determine tracking error rate information from the tracking error display. A system disturbance, composed of a sum of sinusoids, was applied as a velocity disturbance for the velocity and acceleration command tasks and as a position disturbance for the position command task. The amplitudes of the sine waves were chosen to simulate a first-order noise spectrum for the velocity disturbance and a second-order noise spectrum for the position disturbance, both with a break frequency of 2 rad/sec. In these tracking tasks, the human controller was instructed to minimize mean-square tracking error. A more complete description of the experimental setup is given in Kleinman, Baron, and Levison 1970 and Baron et al. 1970.

5.2. Task Modelling

For the pilot modelling analysis of the three tracking experiments, the pilot's objective function J_p was modelled as

$$J_p = E_\infty \left\{ e^2 + f\dot{\delta}^2 \right\} \tag{5.1}$$

where e is pilot tracking error. The system input disturbances were modelled as a white noise process passed through a first-order low pass filter for the velocity and acceleration command dynamics and passed through a second-order low pass filter for the position command dynamics.

A summary of the pilot model input parameters for analysis of each of the plant dynamics is presented in table I. Identical values were used for the analysis performed with the OCM and LQG models. For the Hess model, identical input values were used with the exception of control weighting, which was chosen to match the rms error statistics of the experimental data. Since this is a single-axis task using a single display indicator, the effects of attention allocation and thresholds were assumed small and were not modelled.

Table I. Pilot Model Input Parameters

Input parameter	Velocity command	Acceleration command	Position command
Effective time delay, τ	0.15 sec	0.21 sec	0.15 sec
Neuromotor lag,[a] τ_η	0.08 sec	0.1 sec	0.11 sec
Observation noise ratio, ρ_y	-20 dB	-20 dB	-20 dB
Motor noise ratio, ρ_u	-25 dB	-25 dB	-25 dB
System disturbance	$\frac{v_{\text{dist}}}{w} = \frac{1}{s+2}$	$\frac{v_{\text{dist}}}{w} = \frac{1}{s+2}$	$\frac{x_{\text{dist}}}{w} = \frac{1}{s^2+4s+4}$
Disturbance intensity, $\mathbf{W}$	8.8	0.217	10.0
Objective function observation weights, $\mathbf{Q}_y$	diag(1,0)	diag(1,0)	diag(1,0)
Objective function input weights, r	[b]0, 0, 0, 0.034	[b]0, 0, 0, 0.01	[b]0, 0, 0, 0.0012

[a]Cost function weighting f is chosen to achieve desired τ_η in MOCM, OCM, and LQOCM.
[b]MOCM, OCM, LQOCM, HOCM.

5.2.1. Velocity command system.

The dynamics of the system to be controlled in transfer function form are given by

$$\frac{\theta}{\delta} = \frac{k}{s} \tag{5.2}$$

with $k = 1$. The velocity disturbance was modelled by white noise passed through a first-order filter with a break frequency of 2 rad/sec:

$$\frac{v_{\text{dist}}}{w} = \frac{1}{s+2} \tag{5.3}$$

In state space form, the combined plant and disturbance dynamics, expressed in terms of system disturbance and command tracking error, are given by

$$\frac{d}{dt} \left\{ \begin{matrix} v_{\text{dist}} \\ e \end{matrix} \right\} = \begin{bmatrix} -2 & 0 \\ 1 & 0 \end{bmatrix} \left\{ \begin{matrix} v_{\text{dist}} \\ e \end{matrix} \right\} + \begin{bmatrix} 0 \\ 1 \end{bmatrix} \delta + \begin{bmatrix} 1 \\ 0 \end{bmatrix} w \tag{5.4}$$

The observed system outputs are given by

$$\mathbf{y}_{\text{obs}} = \left\{ \begin{matrix} e \\ \dot{e} \end{matrix} \right\} = \begin{bmatrix} 0 & 1 \\ 1 & 0 \end{bmatrix} \left\{ \begin{matrix} v_{\text{dist}} \\ e \end{matrix} \right\} + \begin{bmatrix} 0 \\ 1 \end{bmatrix} \delta + \mathbf{v}_y$$

where e and $\dot{e}$ are pilot tracking error and pilot tracking error rate, respectively.

11

With the MOCM, a transfer function description of the human pilot's compensation can be determined directly from the state space description, relating the two inputs to the pilot, e and $\dot{e}$, to the single output, δ, as follows:

$$\delta = H_{\delta e} e + H_{\delta\dot{e}}\dot{e} \tag{5.5}$$

where $H_{\delta e}$ and $H_{\delta\dot{e}}$ are pilot tracking error to δ and pilot tracking error rate to δ transfer functions, respectively. Since the $H_{\delta e}$ and $H_{\delta\dot{e}}$ transfer functions are not directly measurable, an equivalent transfer function must be formed for comparison with the measured data. The equivalent pilot transfer function is given by

$$\frac{\delta}{e} = H_{\delta e} + s H_{\delta\dot{e}} \tag{5.6}$$

5.2.2. Acceleration command system. For the acceleration command system, the dynamics of the system to be controlled, in transfer function form, are given by

$$\frac{\theta}{\delta} = \frac{k}{s^2} \tag{5.7}$$

with $k = 1$. The disturbance to the system was modelled as a velocity disturbance by passing white noise through a first-order filter with a break frequency at 2 rad/sec:

$$\frac{v_{\text{dist}}}{w} = \frac{1}{s+2}$$

In state space form, the combined plant and disturbance dynamics are given by

$$\frac{d}{dt} \left\{ \begin{array}{c} v_{\text{dist}} \\ e \\ x_3 \end{array} \right\} = \begin{bmatrix} -2 & 0 & 0 \\ 1 & 0 & 1 \\ 0 & 0 & 0 \end{bmatrix} \left\{ \begin{array}{c} v_{\text{dist}} \\ e \\ x_3 \end{array} \right\} + \begin{bmatrix} 0 \\ 0 \\ 1 \end{bmatrix} \delta + \begin{bmatrix} 1 \\ 0 \\ 0 \end{bmatrix} w \tag{5.8}$$

The observed system outputs are

$$\mathbf{y}_{\text{obs}} = \left\{ \begin{array}{c} e \\ \dot{e} \end{array} \right\} = \begin{bmatrix} 0 & 1 & 0 \\ 1 & 0 & 1 \end{bmatrix} \left\{ \begin{array}{c} v_{\text{dist}} \\ e \\ x_3 \end{array} \right\} + \mathbf{v}_y$$

where x_i is a plant state.

5.2.3. Position command system. In order to reduce high frequency noise, the pure gain dynamics of the position command system were approximated by a low pass filter with a break frequency at 40 rad/sec. Therefore, the plant dynamics to be controlled are given by

$$\frac{\theta}{\delta} = \frac{40}{s+40} \tag{5.9}$$

The position disturbance was modelled by white noise passed through a second-order filter with a break frequency of 2 rad/sec and a damping of unity:

$$\frac{x_{\text{dist}}}{w} = \frac{1}{s^2 + 4s + 4} \tag{5.10}$$

12

In state space form the combined plant and disturbance dynamics are given by

$$\frac{d}{dt}\left\{\begin{array}{c} x_{dist_1} \\ x_{dist_2} \\ x_3 \end{array}\right\} = \begin{bmatrix} 0 & 1 & 0 \\ -4 & -4 & 0 \\ 0 & 0 & -40 \end{bmatrix} \left\{\begin{array}{c} x_{dist_1} \\ x_{dist_2} \\ x_3 \end{array}\right\} + \begin{bmatrix} 0 \\ 0 \\ 40 \end{bmatrix}\delta + \begin{bmatrix} 0 \\ 1 \\ 0 \end{bmatrix}w \qquad (5.11)$$

The observed system outputs are

$$\mathbf{y}_{obs} = \left\{\begin{array}{c} e \\ \dot{e} \end{array}\right\} = \begin{bmatrix} 1 & 0 & 1 \\ 0 & 1 & -40 \end{bmatrix}\left\{\begin{array}{c} x_{dist_1} \\ x_{dist_2} \\ x_3 \end{array}\right\} + \begin{bmatrix} 0 \\ 40 \end{bmatrix}\delta + \mathbf{v}_y$$

where x_{dist_i} is a disturbance state and x_3 is a plant state.

5.3. Discussion of Examples

The measured human-describing functions and model-based analysis results obtained for the velocity command system are given in figure 3. For this command system, the MOCM provides a very good prediction of the measured magnitude and phase in the frequency range from approximately 1 to 30 rad/sec. Note also that the MOCM prediction provides an accurate modelling of the pilot's neuromotor resonant peak. The measured human-describing functions and analysis results obtained for the acceleration command system are given in figure 4. The MOCM

Figure 3. Measured human-describing functions and model-based pilot transfer functions for velocity command system. Measured data from Kleinman, Baron, and Levison 1970.

Figure 4. Measured human-describing functions and model-based pilot transfer functions for acceleration command system. Measured data from Kleinman, Baron, and Levison 1970.

provides a very good prediction of the measured magnitude and phase in the frequency range from approximately 1 to 20 rad/sec. The measured human-describing functions and model-based analysis results obtained for the position command system are given in figure 5. For this command system, the MOCM provides a fair prediction of the measured magnitude and a very good prediction of the measured phase in the frequency range from approximately 1 to 20 rad/sec. As can be seen from figures 3 through 5 the model-based pilot transfer functions obtained with the MOCM compare very favorably with the predictions of the OCM for each command system. Also, overall the MOCM provides a better match to the measured human-describing functions than either the LQG model or the Hess model for the given pilot model input parameters. (The reader should note that a better match to the measured human-describing functions may be possible with the LQG and Hess models by varying the pilot model input parameters.)

Measured and model-based rms pilot performance is presented in table II. As can be seen, the model-based rms pilot performance obtained from the MOCM analysis is in good agreement with the measured rms statistics for each task. The OCM also provides a favorable match to the measured rms performance. Pilot transfer functions obtained from the MOCM analysis are presented in table III.

The effect on the pilot transfer function for the velocity command system of replacing the MOCM's modelling of the pilot's effective time delay (a second-order Pade approximation) with a first- and third-order Pade approximation is presented in figure 6. As can be seen, at least
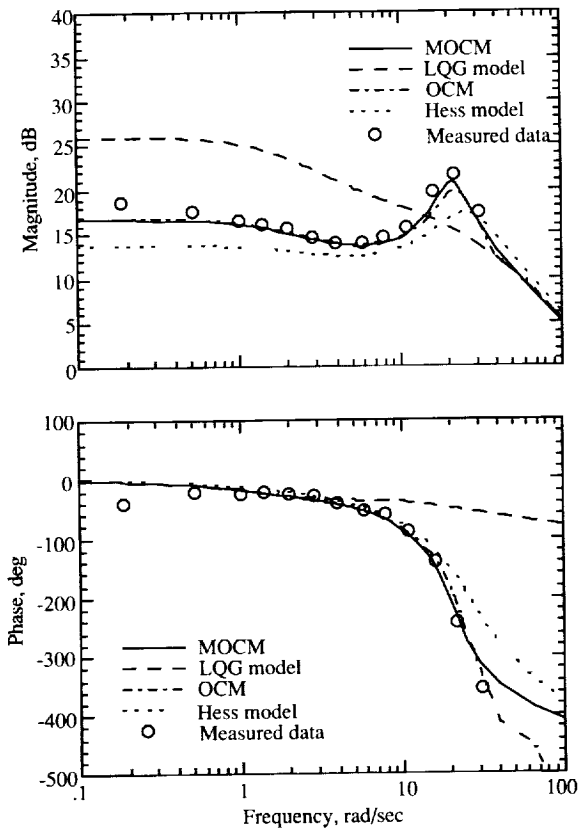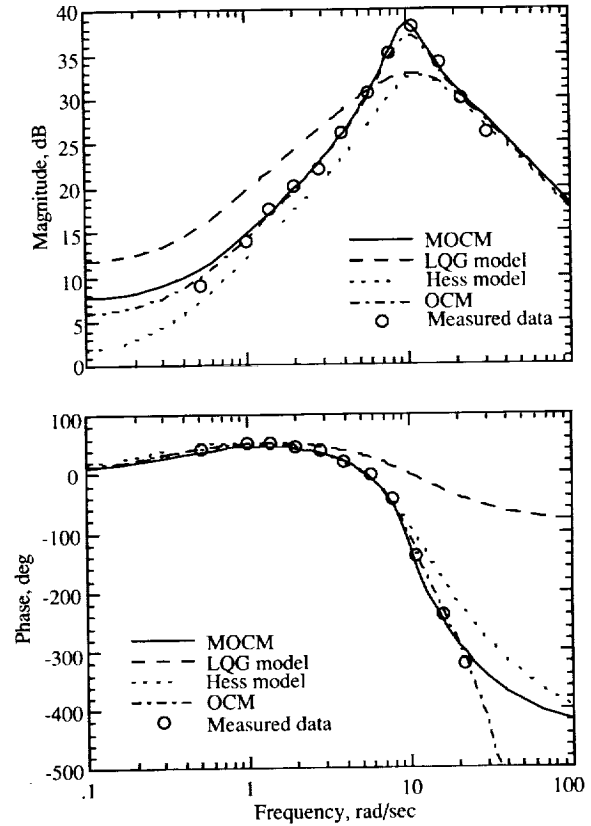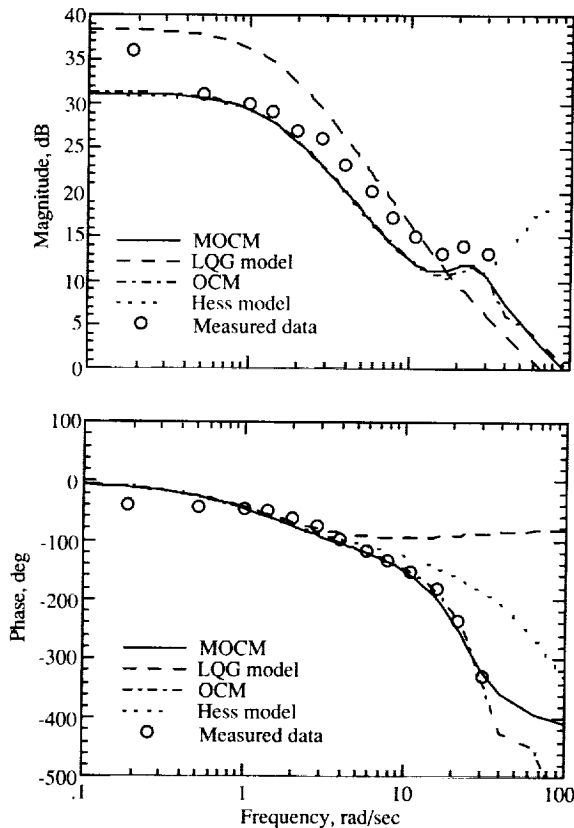

Figure 5. Measured human-describing functions and model-based pilot transfer functions for position command system. Measured data from Kleinman, Baron, and Levison 1970.
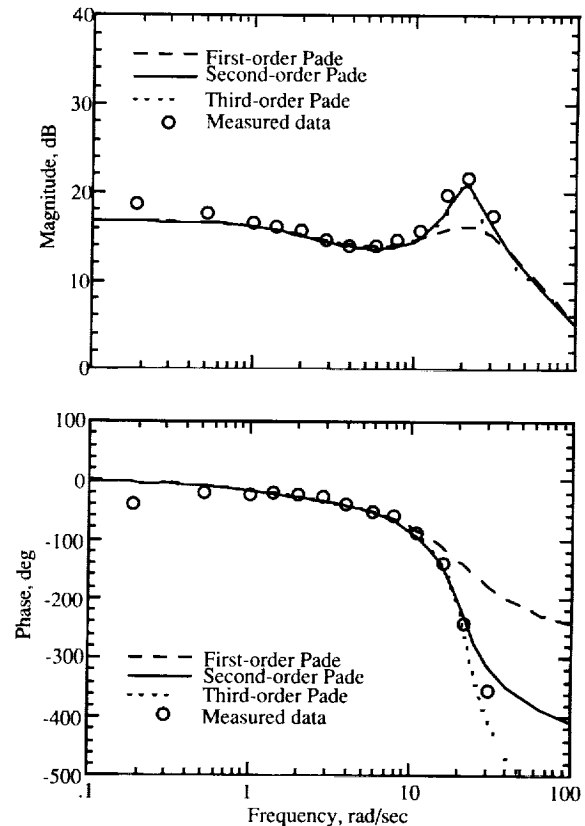
Figure 6. Modelling pilot's effective time delay by various Pade approximations and measured human-describing functions for velocity command system. Measured data from Kleinman, Baron, and Levison 1970.

a second-order Pade approximation is required to capture the pilot's high frequency dynamic compensation characteristics in this task. This tends to suggest a connection between the pilot's effective time delay and high frequency neuromotor resonant peak.

Table II. Measured and Model-Based rms Pilot Performance

Data	Velocity command			Acceleration command			Position command		
	Error	Error rate	Control	Error	Error rate	Control	Error	Error rate	Control
Measured[a]	0.36	1.76	2.05	0.12	0.32	1.20	0.36	2.19	0.73
MOCM	0.34	1.75	1.97	0.12	0.33	1.17	0.27	2.26	0.47
OCM	0.34	1.72	1.94	0.11	0.32	1.07	0.27	2.28	0.47
LQG model	0.14	1.03	1.63	0.07	0.23	0.87	0.16	2.22	0.52
Hess model	0.36	1.53	1.70	0.12	0.28	0.68	0.36	6.14	0.55

[a]Measured rms pilot performance data taken from Kleinman, Baron, and Levison 1970.

Table III. Summary of MOCM Pilot Transfer Functions

Command	Model-based pilot transfer functions (a)
Velocity	$\dfrac{\delta}{e} = \dfrac{181.2(3.26)(6.37)(12.74)(-0.707,18.86)}{(1.99)(6.44)(12.49)(0.264,20.99)(35.33)}$
Acceleration	$\dfrac{\delta}{e} = \dfrac{443.3(0.47)(2.32)(3.29)(10.03)(-0.707,13.47)}{(2.00)(3.22)(9.99)(0.256,10.08)(0.820,18.22)}$
Position	$\dfrac{\delta}{e} = \dfrac{10.19(4.14)(9.14)(11.55)(-0.707,18.86)(40.70)}{(1.45)(2.80)(9.10)(11.37)(0.389,24.76)(71.65)}$

[a]( ) = Real pole or Zero; (,) = (ξ, ω) = Damping and Frequency of complex pole or zero pair.

6. Concluding Remarks

This paper has presented a modified optimal control model (MOCM) based upon the optimal control model (OCM) developed by Kleinman, Baron, and Levison (*Automatica*, May 1970). This model is input compatible with the OCM and retains other key aspects of the OCM, such as the linear quadratic solution for the pilot gains with inclusion of control rate in the cost function, a Kalman estimator, and the ability to account for attention allocation and perception threshold effects. An algorithm designed for easy implementation in current dynamic systems analysis and design software has been presented. Implementation in this type of environment allows for rapid calculation of pilot and system transfer function descriptions from state space models, determination of system frequency responses, and ease of system state space and frequency representations.

The MOCM was used to predict closed-loop pilot performance in a compensatory tracking task for three basic dynamic systems. These predictions were compared with measured pilot performance and shown to provide a very good modelling of both pilot-describing functions and time domain performance statistics for these dynamic systems. Also, the predicted models obtained with the MOCM were compared with similar analyses performed with the OCM and two previously proposed LQG (linear quadratic Gaussian) based pilot models—an LQG approximation to the OCM and a model proposed by Hess. The MOCM is shown to provide results very similar to those of the OCM and to compare more favorably with the measured pilot performance than the other pilot model predictions.

In this formulation, use of at least a second-order Pade approximation is required in order to accurately model pilot magnitude and phase compensation at the high end of the pilot's bandwidth, such as the pilot high frequency neuromotor resonant peak. This tends to suggest a connection between the pilot's effective time delay and high frequency neuromotor resonant peak.

NASA Langley Research Center
Hampton, VA 23681-0001
August 13, 1992

Appendix A

Modified Optimal Control Pilot Model Flowchart


```
┌─────────────────────────────┐
│     Load system matrices    │
│        (eqs. (4.1))         │
│            and              │
│   pilot control parameters  │
│      (see table I)          │
└─────────────────────────────┘
               │
               ▼
┌─────────────────────────────┐
│  Augment system matrices    │
│       with delay dynamics   │
│        (eqs. (4.4))         │
└─────────────────────────────┘
               │
               ▼
┌─────────────────────────────┐
│     Create control-rate     │
│         formulation         │
│        (eqs. (4.6))         │
└─────────────────────────────┘
               │
               ▼
┌─────────────────────────────┐      ┌─────────────────────────┐
│    Calculate pilot gains    │◄─────│   Adjust control-rate    │
│   (eqs. (4.7) and (4.8))    │      │        weighting         │
└─────────────────────────────┘      │       (eq. (4.5))        │
               │                     └─────────────────────────┘
               ▼                                  ▲
          ╱─────────╲                             │
        ╱  Achieved   ╲                           │
       ╱   desired      ╲                         │
      ╱  value of         ╲─── No ────────────────┘
       ╲  neuromotor     ╱
        ╲    lag?      ╱
          ╲─────────╱
               │
              Yes
               │
               ▼
┌─────────────────────────────┐
│  Augment system with lag    │
│         dynamics            │
│       (eqs. (4.14))         │
└─────────────────────────────┘
               │
               ▼
```

```
                    │
                    ▼
        ┌──────────────────────────┐
        │ Generate initial guess for observation │
        │   and control noise intensities        │
        └──────────────────────────┘
                    │
                    ▼
        ┌──────────────────────────┐
        │   Calculate effects of fractions of    │◄─────────────┐
        │    attentions and thresholds on        │              │
        │         observation noise              │              │
        │           (eq. (4.19))                 │              │
        └──────────────────────────┘              │
                    │                              │
                    ▼                              │
        ┌──────────────────────────┐              │
        │     Calculate estimator gains          │   ┌──────────────────────────┐
        │     (eqs. (4.15) and (4.16))           │   │ Adjust values of observation and │
        └──────────────────────────┘   │    control noise intensities     │
                    │                      └──────────────────────────┘
                    ▼                              ▲
        ┌──────────────────────────┐              │
        │       Form closed-loop system          │              │
        │           (eqs. (4.17))                │              │
        └──────────────────────────┘              │
                    │                              │
                    ▼                              │
        ┌──────────────────────────┐              │
        │   Calculate achieved observation and   │              │
        │     control noise-to-signal ratios     │              │
        └──────────────────────────┘              │
                    │                              │
                    ▼                              │
              ╱─────────╲                          │
             ╱ Achieved  ╲                         │
            ╱  desired    ╲        No              │
            ╲noise-to-signal╲──────────────────────┘
             ╲  ratios?    ╱
              ╲─────────╱
                    │
                   Yes
                    │
                    ▼
```

```
┌─────────────────────────────────┐
│   Calculate closed-loop eigenvalues  │
│        and rms output values         │
└─────────────────────────────────┘
                  │
                  ▼
┌─────────────────────────────────┐
│        Form pilot matrices          │
│          (eqs. (4.18))              │
└─────────────────────────────────┘
                  │
                  ▼
┌─────────────────────────────────┐
│   Generate system and pilot frequency │
│    responses and transfer functions   │
└─────────────────────────────────┘
                  │
                  ▼
╭─────────────────────────────────╮
│     Adjust input parameters and      │
│      reanalyze or end analysis       │
╰─────────────────────────────────╯
```

Appendix B

LQG Approximation to Optimal Pilot Model

This appendix presents a theoretical development of an LQG approximation to the optimal pilot model (Schmidt 1979). The plant dynamics to be controlled, augmented with the disturbance dynamics, are given by the state space time invariant linear equations

$$\left.\begin{array}{c} \dot{\mathbf{x}} = \mathbf{A}\mathbf{x} + \mathbf{B}\delta + \mathbf{E}\mathbf{w} \\ \mathbf{y} = \mathbf{C}\mathbf{x} + \mathbf{D}\delta \end{array}\right\} \tag{B1}$$

where $\mathbf{x}(t)$ is an n-dimensional state vector, $\delta(t)$ is an n_u-dimensional vector of pilot inputs, $\mathbf{w}(t)$ is an n_w-dimensional disturbance vector modelled as zero mean Gaussian white noise with covariance $\mathbf{W}$, and $\mathbf{y}(t)$ is an n_y-dimensional output vector. The vector $\mathbf{y}_{\text{obs}}(t)$, of dimension n_y, represents variables the pilot can perceive, either by observation or feel. The outputs observed by the pilot are assumed to be corrupted by an observation noise $\mathbf{v}_y(t)$, a zero mean Gaussian white noise process with covariance $\mathbf{V}_y$, as follows:

$$\mathbf{y}_{\text{obs}} = \mathbf{C}\mathbf{x} + \mathbf{D}\delta + \mathbf{v}_y$$

The following development considers the case of a scalar pilot input δ.

The pilot's control task is assumed to be modelled as the minimization of the quadratic performance index J_p given by

$$J_p = E_\infty \left\{ \mathbf{y}^T \mathbf{Q}_y \mathbf{y} + \delta^T r \delta + \dot{\delta}^T f \dot{\delta} \right\} \tag{B2}$$

subject to pilot observations $\mathbf{y}_{\text{obs}}$ with cost functional weightings $\mathbf{Q}_y \geq 0$, $r \geq 0$, and $f > 0$. By defining a new state vector as

$$\chi^T = [\mathbf{x} \quad \delta]^T$$

the augmented system can be expressed in a control-rate formulation as

$$\left.\begin{array}{c} \frac{d}{dt}\left\{\begin{array}{c} \mathbf{x} \\ \delta \end{array}\right\} = \left[\begin{array}{cc} \mathbf{A} & \mathbf{B} \\ 0 & 0 \end{array}\right]\left\{\begin{array}{c} \mathbf{x} \\ \delta \end{array}\right\} + \left[\begin{array}{c} 0 \\ 1 \end{array}\right]\dot{\delta} + \left[\begin{array}{c} \mathbf{E} \\ 0 \end{array}\right]\mathbf{w} \\ \mathbf{y} = [\mathbf{C} \quad \mathbf{D}]\left\{\begin{array}{c} \mathbf{x} \\ \delta \end{array}\right\} \end{array}\right\} \tag{B3a}$$

or

$$\left.\begin{array}{c} \dot{\chi} = \mathbf{A}_o\chi + \mathbf{B}_o\dot{\delta} + \mathbf{E}_o\mathbf{w} \\ \mathbf{y} = \mathbf{C}_o\chi \\ \mathbf{y}_{\text{obs}} = \mathbf{C}_o\chi + \mathbf{v}_y \end{array}\right\} \tag{B3b}$$

The minimizing control law is obtained by application of LQG solution techniques to the augmented system. This leads to the full-state feedback relation

$$\dot{\delta} = -\mathbf{g}_p\widehat{\chi} = -[g_1, \ldots, g_n, g_{n+1}]\widehat{\chi} = -f^{-1}(\mathbf{B}_o)^T \mathbf{K}\widehat{\chi} \tag{B4}$$

where $\widehat{\chi}$ is the estimate of the state χ and $\mathbf{K}$ is the unique positive definite solution of the matrix Ricatti equation

$$0 = (\mathbf{A}_o)^T \mathbf{K} + \mathbf{K}\mathbf{A}_o + \mathbf{Q}_o - \mathbf{K}\mathbf{B}_o f^{-1}(\mathbf{B}_o)^T \mathbf{K} \tag{B5}$$

where

$$\mathbf{Q}_o = \begin{bmatrix} \mathbf{C}^T \mathbf{Q}_y \mathbf{C} & \mathbf{C}^T \mathbf{Q}_y \mathbf{D} \\ \mathbf{D}^T \mathbf{Q}_y \mathbf{C} & \mathbf{D}^T \mathbf{Q}_y \mathbf{D} + r \end{bmatrix}$$

By expanding the optimal control law in terms of $\hat{\mathbf{x}}$ and δ

$$\dot{\delta} = - [g_1, \ldots, g_n] \hat{\mathbf{x}} - g_{n+1} \delta \tag{B6}$$

and letting

$$\tau_\eta = \frac{1}{g_{n+1}}$$

and

$$\mathbf{l}_p = \tau_\eta [g_1, \ldots, g_n]$$

then

$$\tau_\eta \dot{\delta} + \delta = u_c \tag{B7}$$

where the pilot's commanded control u_c is given by

$$u_c = -\mathbf{l}_p \hat{\mathbf{x}} \tag{B8}$$

To account for the uncertainty of the human operator's control input, control noise v_u is added to the commanded control u_c

$$\tau_\eta \dot{\delta} + \delta = u_c + v_u \tag{B9}$$

leading to

$$\dot{\delta} = \frac{-1}{\tau_\eta} \delta + \frac{1}{\tau_\eta} u_c + \frac{1}{\tau_\eta} v_u \tag{B10}$$

where v_u is a zero mean Gaussian white noise process with covariance $\mathbf{V}_u$. By combining this result with the original control-rate formulation, one obtains the augmented system

$$\left. \begin{aligned} \frac{d}{dt} \left\{ \begin{matrix} \mathbf{x} \\ \delta \end{matrix} \right\} &= \begin{bmatrix} \mathbf{A} & \mathbf{B} \\ 0 & -1/\tau_\eta \end{bmatrix} \left\{ \begin{matrix} \mathbf{x} \\ \delta \end{matrix} \right\} + \begin{bmatrix} 0 \\ -1/\tau_\eta \end{bmatrix} u_c + \begin{bmatrix} \mathbf{E} & 0 \\ 0 & 1/\tau_\eta \end{bmatrix} \left\{ \begin{matrix} \mathbf{w} \\ v_u \end{matrix} \right\} \\ \mathbf{y}_{\text{obs}} &= [\mathbf{C} \quad \mathbf{D}] \left\{ \begin{matrix} \mathbf{x} \\ \delta \end{matrix} \right\} + \mathbf{v}_y \end{aligned} \right\} \tag{B11a}$$

or

$$\left. \begin{aligned} \dot{\chi} &= \mathbf{A}_1 \chi + \mathbf{B}_1 u_c + \mathbf{E}_1 \mathbf{w}_1 \\ \mathbf{y}_{\text{obs}} &= \mathbf{C}_1 \chi + \mathbf{v}_y \end{aligned} \right\} \tag{B11b}$$

The current estimate of the state is given by a Kalman filter

$$\left. \begin{aligned} \dot{\hat{\chi}} &= \mathbf{A}_1 \hat{\chi} + \mathbf{B}_1 u_c + \mathbf{F} (\mathbf{y}_{\text{obs}} - \hat{y}) \\ \dot{\hat{\chi}} &= (\mathbf{A}_1 - \mathbf{F}\mathbf{C}_1) \hat{\chi} + \mathbf{F}\mathbf{C}_1 \chi + \mathbf{B}_1 u_c + \mathbf{F}\mathbf{v}_y \end{aligned} \right\} \tag{B12}$$

where

$$\mathbf{F} = \Sigma_1 (\mathbf{C}_1)^T (\mathbf{V}_y)^{-1}$$

The covariance matrix of the estimation error Σ_1 is the unique positive definite solution of the matrix Ricatti equation

$$0 = \mathbf{A}_1 \Sigma_1 + \Sigma_1 (\mathbf{A}_1)^T + \mathbf{W}_1 - \Sigma_1 (\mathbf{C}_1)^T (\mathbf{V}_y)^{-1} \mathbf{C}_1 \Sigma_1 \tag{B13}$$

where $\mathbf{W}_1 = \mathrm{diag}(\mathbf{W}, \mathbf{V}_u)$. A state space representation of the closed-loop system is given by

$$
\left.
\begin{aligned}
\frac{d}{dt}\begin{Bmatrix} \chi \\ \hat{\chi} \end{Bmatrix} &= \begin{bmatrix} \mathbf{A}_1 & -\mathbf{B}_1\mathbf{l}_1 \\ \mathbf{FC}_1 & \mathbf{A}_1 - \mathbf{B}_1\mathbf{l}_1 - \mathbf{FC}_1 \end{bmatrix} \begin{Bmatrix} \chi \\ \hat{\chi} \end{Bmatrix} + \begin{bmatrix} \mathbf{E}_1 & 0 \\ 0 & \mathbf{F} \end{bmatrix} \begin{Bmatrix} \mathbf{w}_1 \\ \mathbf{v}_y \end{Bmatrix} \\
\begin{Bmatrix} \mathbf{y}_{\mathrm{obs}} \\ u_c \end{Bmatrix} &= \begin{bmatrix} \mathbf{C}_1 & 0 \\ 0 & -\mathbf{l}_1 \end{bmatrix} \begin{Bmatrix} \chi \\ \hat{\chi} \end{Bmatrix} + \begin{Bmatrix} \mathbf{v}_y \\ 0 \end{Bmatrix}
\end{aligned}
\right\} \tag{B14}
$$

where $\mathbf{l}_1 = [\mathbf{I}_p \quad 0]$. A state space representation of the pilot's dynamics is given by

$$
\left.
\begin{aligned}
\frac{d}{dt}\begin{Bmatrix} \hat{\chi} \\ \delta \end{Bmatrix} &= \begin{bmatrix} \mathbf{A}_1 - \mathbf{FC}_1 - \mathbf{B}_1\mathbf{l}_1 & 0 \\ -1/\tau_\eta & -1/\tau_\eta \end{bmatrix} \begin{Bmatrix} \hat{\chi} \\ \delta \end{Bmatrix} + \begin{bmatrix} \mathbf{F} \\ 0 \end{bmatrix} \mathbf{y} + \begin{bmatrix} \mathbf{F} & 0 \\ 0 & 1/\tau_\eta \end{bmatrix} \begin{Bmatrix} \mathbf{v}_y \\ v_u \end{Bmatrix} \\
\delta &= [0 \quad 1]\begin{Bmatrix} \hat{\chi} \\ \delta \end{Bmatrix}
\end{aligned}
\right\} \tag{B15a}
$$

or

$$
\left.
\begin{aligned}
\dot{\mathbf{x}}_p &= \mathbf{A}_p\mathbf{x}_p + \mathbf{B}_p\mathbf{y} + \mathbf{E}_p\mathbf{v}_p \\
\delta &= \mathbf{C}_p\mathbf{x}_p
\end{aligned}
\right\} \tag{B15b}
$$

Appendix C

Hess's LQG-Based Pilot Model

This appendix presents a theoretical development of Hess's LQG-based pilot model (Hess 1976). The plant dynamics to be controlled, augmented with the disturbance dynamics, are given by the state space time invariant linear equations

$$
\left.
\begin{aligned}
\dot{\mathbf{x}} &= \mathbf{A}\mathbf{x} + \mathbf{B}\delta + \mathbf{E}\mathbf{w} \\
\mathbf{y} &= \mathbf{C}\mathbf{x} + \mathbf{D}\delta
\end{aligned}
\right\}
\tag{C1}
$$

where $\mathbf{x}(t)$ is an n-dimensional state vector, $\delta(t)$ is an n_u-dimensional vector of pilot inputs, $\mathbf{w}(t)$ is an n_w-dimensional disturbance vector modelled as zero mean Gaussian white noise with covariance $\mathbf{W}$, and $\mathbf{y}(t)$ is an n_y-dimensional vector of outputs. The vector $\mathbf{y}_{\text{obs}}$, of dimension n_y, represents variables the pilot can perceive, either by observation or feel. The outputs observed by the pilot are assumed to be corrupted by an observation noise $\mathbf{v}_y(t)$, a zero mean Gaussian white noise process with intensity $\mathbf{V}_y$:

$$
\mathbf{y}_{\text{obs}} = \mathbf{C}\mathbf{x} + \mathbf{D}\delta + \mathbf{v}_y
$$

The following development is for the case of a scalar pilot input δ.

The pilot's effective time delay is modelled by a second-order transfer function given by

$$
\frac{u_d}{u_c} = \frac{(s - 4/\tau)^2}{(s + 4/\tau)^2}
\tag{C2}
$$

where τ is the delay interval, u_d is the pilot's delayed control input, and u_c is the pilot's commanded control. In state space form, this is expressed as

$$
\left.
\begin{aligned}
\frac{d}{dt}
\begin{Bmatrix} \mathbf{x}_{d1} \\ \mathbf{x}_{d2} \end{Bmatrix}
&=
\begin{bmatrix} 0 & -16/\tau^2 \\ 1 & -8/\tau \end{bmatrix}
\begin{Bmatrix} \mathbf{x}_{d1} \\ \mathbf{x}_{d2} \end{Bmatrix}
+
\begin{bmatrix} 0 \\ -16/\tau \end{bmatrix} u_c \\
u_d &=
\begin{bmatrix} 0 & 1 \end{bmatrix}
\begin{Bmatrix} \mathbf{x}_{d1} \\ \mathbf{x}_{d2} \end{Bmatrix}
+ u_c
\end{aligned}
\right\}
\tag{C3}
$$

where $\mathbf{x}_{di}$ is a delay state.

To account for the uncertainty of the human operator's control input, control noise is added to the pilot's delayed control input

$$
u_n = u_d + v_u
\tag{C4}
$$

where v_u is a zero mean Gaussian white noise process with covariance $\mathbf{V}_u$.

The pilot's neuromotor dynamics are modelled as a first-order lag given by

$$
\frac{\delta}{u_n} = \frac{1}{\tau_\eta s + 1}
\tag{C5}
$$

The effective time delay and first-order neuromotor lag are placed at the pilot's output and are treated as part of the plant dynamics for determination of the pilot's regulation and filter gains.

The combined time delay and lag dynamics, in state space form, are given by

$$\frac{d}{dt}\begin{Bmatrix} \mathbf{x}_{d1} \\ \mathbf{x}_{d2} \\ \delta \end{Bmatrix} = \begin{bmatrix} 0 & -16/\tau^2 & 0 \\ 1 & -8/\tau & 0 \\ 0 & 1/\tau_\eta & -1/\tau_\eta \end{bmatrix} \begin{Bmatrix} \mathbf{x}_{d1} \\ \mathbf{x}_{d2} \\ \delta \end{Bmatrix} + \begin{bmatrix} 0 \\ -16/\tau \\ 1/\tau_\eta \end{bmatrix} u_c + \begin{bmatrix} 0 \\ 0 \\ 1/\tau_\eta \end{bmatrix} v_u$$

$$\delta = \begin{bmatrix} 0 & 0 & 1 \end{bmatrix} \begin{Bmatrix} \mathbf{x}_{d1} \\ \mathbf{x}_{d2} \\ \delta \end{Bmatrix} \qquad \text{(C6a)}$$

or

$$\dot{\mathbf{x}}_d = \mathbf{A}_d \mathbf{x}_d + \mathbf{B}_d u_c + \mathbf{E}_d v_u$$
$$\delta = \mathbf{C}_d \mathbf{x}_d \qquad \text{(C6b)}$$

The plant, augmented with the neuromotor lag and effective time delay dynamics, is given by

$$\frac{d}{dt}\begin{Bmatrix} \mathbf{x} \\ \mathbf{x}_d \end{Bmatrix} = \begin{bmatrix} \mathbf{A} & \mathbf{BC}_d \\ 0 & \mathbf{A}_d \end{bmatrix} \begin{Bmatrix} \mathbf{x} \\ \mathbf{x}_d \end{Bmatrix} + \begin{bmatrix} 0 \\ \mathbf{B}_d \end{bmatrix} u_c + \begin{bmatrix} \mathbf{E} & 0 \\ 0 & \mathbf{E}_d \end{bmatrix} \begin{Bmatrix} \mathbf{w} \\ v_u \end{Bmatrix}$$

$$\mathbf{y} = \begin{bmatrix} \mathbf{C} & \mathbf{DC}_d \end{bmatrix} \begin{Bmatrix} \mathbf{x} \\ \mathbf{x}_d \end{Bmatrix} \qquad \text{(C7a)}$$

or

$$\dot{\mathbf{x}}_s = \mathbf{A}_s \mathbf{x}_s + \mathbf{B}_s u_c + \mathbf{E}_s \mathbf{w}_1$$
$$\mathbf{y} = \mathbf{C}_s \mathbf{x}_s$$
$$\mathbf{y}_{\text{obs}} = \mathbf{C}_s \mathbf{x}_s + \mathbf{v}_y \qquad \text{(C7b)}$$

The pilot's control task is assumed to be modelled as the minimization of the quadratic performance index J_p given by

$$J_p = E_\infty \left\{ \mathbf{y}^T \mathbf{Q}_y \mathbf{y} + (u_c)^T r u_c \right\} \qquad \text{(C8)}$$

subject to pilot observations $\mathbf{y}_{\text{obs}}$, with cost function weights $\mathbf{Q}_y \geq 0$ and $r > 0$. The minimizing control law is obtained by application of LQG solution techniques to the augmented system. This leads to the full-state feedback relation

$$u_c = -\mathbf{g}_p \hat{\mathbf{x}}_s = -r^{-1} (\mathbf{B}_s)^T \mathbf{K} \hat{\mathbf{x}}_s \qquad \text{(C9)}$$

where $\hat{\mathbf{x}}_s$ is the estimate of the state $\mathbf{x}_s$ and $\mathbf{K}$ is the unique positive definite solution of the matrix Ricatti equation

$$0 = (\mathbf{A}_s)^T \mathbf{K} + \mathbf{K}\mathbf{A}_s + \mathbf{Q} - \mathbf{K}\mathbf{B}_s r^{-1} (\mathbf{B}_s)^T \mathbf{K} \qquad \text{(C10)}$$

where $\mathbf{Q} = \mathbf{C}_s^T \mathbf{Q}_y \mathbf{C}_s$.

The current estimate of the state is given by a Kalman filter

$$\dot{\hat{\mathbf{x}}}_s = \mathbf{A}_s \hat{\mathbf{x}}_s + \mathbf{B}_s u_c + \mathbf{F} (\mathbf{y}_{\text{obs}} - \hat{\mathbf{y}})$$
$$\dot{\hat{\mathbf{x}}}_s = (\mathbf{A}_s - \mathbf{F}\mathbf{C}_s) \hat{\mathbf{x}}_s + \mathbf{F}\mathbf{C}_s \mathbf{x}_s + \mathbf{B}_s u_c + \mathbf{F}\mathbf{v}_y \qquad \text{(C11)}$$

where

$$\mathbf{F} = \mathbf{\Sigma} (\mathbf{C}_s)^T \mathbf{V}_y^{-1}$$

The covariance matrix of the estimation error Σ is the unique positive definite solution of the matrix Ricatti equation

$$0 = \mathbf{A}_s \Sigma + \Sigma (\mathbf{A}_s)^T + \mathbf{W}_1 - \Sigma (\mathbf{C}_s)^T \mathbf{V}_y^{-1} \mathbf{C}_s \Sigma \tag{C12}$$

where $\mathbf{W}_1 = \mathrm{diag}(\mathbf{W}, \mathbf{V}_u)$.

A state space representation of the closed-loop system is given by

$$\left. \begin{aligned} \frac{d}{dt} \left\{ \begin{array}{c} \mathbf{x}_s \\ \hat{\mathbf{x}}_s \end{array} \right\} &= \left[\begin{array}{cc} \mathbf{A}_s & -\mathbf{B}_s \mathbf{g}_p \\ \mathbf{FC}_s & \mathbf{A}_s - \mathbf{B}_s \mathbf{g}_p - \mathbf{FC}_s \end{array} \right] \left\{ \begin{array}{c} \mathbf{x}_s \\ \hat{\mathbf{x}}_s \end{array} \right\} + \left[\begin{array}{cc} \mathbf{E}_s & 0 \\ 0 & \mathbf{F} \end{array} \right] \left\{ \begin{array}{c} \mathbf{w}_1 \\ \mathbf{v}_y \end{array} \right\} \\ \left\{ \begin{array}{c} \mathbf{y}_{\mathrm{obs}} \\ u_c \end{array} \right\} &= \left[\begin{array}{cc} \mathbf{C}_s & 0 \\ 0 & -\mathbf{g}_p \end{array} \right] \left\{ \begin{array}{c} \mathbf{x}_s \\ \hat{\mathbf{x}}_s \end{array} \right\} + \left[\begin{array}{c} \mathbf{v}_y \\ 0 \end{array} \right] \end{aligned} \right\} \tag{C13}$$

A state space representation of the pilot's dynamics is given by

$$\left. \begin{aligned} \frac{d}{dt} \left\{ \begin{array}{c} \hat{\mathbf{x}}_s \\ \mathbf{x}_d \end{array} \right\} &= \left[\begin{array}{cc} \mathbf{A}_s - \mathbf{B}_s \mathbf{g}_p - \mathbf{FC}_s & 0 \\ -\mathbf{B}_d \mathbf{g}_p & \mathbf{A}_d \end{array} \right] \left\{ \begin{array}{c} \hat{\mathbf{x}}_s \\ \mathbf{x}_d \end{array} \right\} + \left[\begin{array}{c} \mathbf{F} \\ 0 \end{array} \right] \mathbf{y} + \left[\begin{array}{cc} \mathbf{F} & 0 \\ 0 & \mathbf{E}_d \end{array} \right] \left\{ \begin{array}{c} \mathbf{v}_y \\ v_u \end{array} \right\} \\ \delta &= \left[\begin{array}{cc} 0 & \mathbf{C}_d \end{array} \right] \left\{ \begin{array}{c} \hat{\mathbf{x}}_s \\ \mathbf{x}_d \end{array} \right\} \end{aligned} \right\} \tag{C14a}$$

or

$$\left. \begin{aligned} \dot{\mathbf{x}}_p &= \mathbf{A}_p \mathbf{x}_p + \mathbf{B}_p \mathbf{y} + \mathbf{E}_p v_p \\ \delta &= \mathbf{C}_p \mathbf{x}_p \end{aligned} \right\} \tag{C14b}$$

References

Anderson, Mark R.; and Schmidt, David K. 1987: Closed-Loop Pilot Vehicle Analysis of the Approach and Landing Task. *J. Guid., Control, & Dyn.*, vol. 10, no. 2, pp. 187–194.

Bacon, Barton J.; and Schmidt, David K. 1983: An Optimal Control Approach to Pilot/Vehicle Analysis and the Neal-Smith Criteria. *J. Guid., Control, & Dyn.*, vol. 6, no. 5, pp. 339–347.

Baron, S.; Kleinman, D. L.; and Levison, W. H. 1970: An Optimal Control Model of Human Response—Part II: Prediction of Human Performance in a Complex Task. *Automatica*, vol. 6, no. 3, pp. 371–383.

Baron, Sheldon; Kleinman, David L.; Miller, Duncan C.; Levison, William H.; and Elkind, Jerome I. 1970: Application of Optimal Control Theory to Prediction of Human Performance in a Complex Task. *Fifth Annual NASA-University Conference on Manual Control*, NASA SP-215, pp. 367–387.

Broussard, John R.; and Stengel, Robert F. 1977: Stability of the Pilot-Aircraft System in Maneuvering Flight. *J. Aircr.*, vol. 14, no. 10, pp. 959–965.

Elkind, J. I. 1964: A Survey of the Development of Models for the Human Controller. *Guidance and Control—II*, Robert C. Langford and Charles J. Mundo, eds., Academic Press, pp. 623–643.

Hess, Ronald A. 1976: *A Method for Generating Numerical Pilot Opinion Ratings Using the Optimal Pilot Model.* NASA TM X-73,101.

Innocenti, Mario 1988: The Optimal Control Pilot Model and Applications. *Advances in Flying Qualities*, AGARD-LS-157, pp. 7-1–7-17.

Kleinman, D. L.; Baron, S.; and Levison, W. H. 1970: An Optimal Control Model of Human Response—Part 1: Theory and Validation. *Automatica*, vol. 6, no. 3, pp. 357–369.

Kwakernaak, Huibert; and Sivan, Raphael 1972: *Linear Optimal Control Systems.* John Wiley & Sons, Inc.

McRuer, D. 1980: Human Dynamics in Man-Machine Systems. *Automatica*, vol. 16, no. 3, pp. 237–253.

Schmidt, David K. 1979: Optimal Flight Control Synthesis Via Pilot Modeling. *J. Guid. & Control*, vol. 2, no. 4, pp. 308–312.

Schmidt, David K. 1981: On the Use of the OCM's Quadratic Objective Function as a Pilot Rating Metric. *Proceedings of the Seventeenth Annual Conference on Manual Control*, JPL Publ. 81-95, pp. 305–313. (Available as NASA CR-165005.)

REPORT DOCUMENTATION PAGE

Public reporting burden for this collection of information is estimated to average 1 hour per response, including the time for reviewing instructions, searching existing data sources, gathering and maintaining the data needed, and completing and reviewing the collection of information. Send comments regarding this burden estimate or any other aspect of this collection of information, including suggestions for reducing this burden, to Washington Headquarters Services, Directorate for Information Operations and Reports, 1215 Jefferson Davis Highway, Suite 1204, Arlington, VA 22202-4302, and to the Office of Management and Budget, Paperwork Reduction Project (0704-0188), Washington, DC 20503.

1. AGENCY USE ONLY *(Leave blank)*	2. REPORT DATE October 1992	3. REPORT TYPE AND DATES COVERED Technical Memorandum

4. TITLE AND SUBTITLE
Modified Optimal Control Pilot Model for Computer-Aided Design and Analysis

5. FUNDING NUMBERS
WU 505-64-30-01

6. AUTHOR(S)
John B. Davidson and David K. Schmidt

7. PERFORMING ORGANIZATION NAME(S) AND ADDRESS(ES)
NASA Langley Research Center
Hampton, VA 23681-0001

8. PERFORMING ORGANIZATION REPORT NUMBER
L-16979

9. SPONSORING/MONITORING AGENCY NAME(S) AND ADDRESS(ES)
National Aeronautics and Space Administration
Washington, DC 20546-0001

10. SPONSORING/MONITORING AGENCY REPORT NUMBER
NASA TM-4384

11. SUPPLEMENTARY NOTES
Davidson: Langley Research Center, Hampton, VA; Schmidt: Arizona State University, Tempe, AZ.

12a. DISTRIBUTION/AVAILABILITY STATEMENT

Unclassified Unlimited

Subject Category 08

12b. DISTRIBUTION CODE

13. ABSTRACT *(Maximum 200 words)*

This paper presents the theoretical development of a modified optimal control pilot model based upon the optimal control model (OCM) of the human operator developed by Kleinman, Baron, and Levison. This model is input compatible with the OCM and retains other key aspects of the OCM, such as a linear quadratic solution for the pilot gains with inclusion of control rate in the cost function, a Kalman estimator, and the ability to account for attention allocation and perception threshold effects. An algorithm designed for easy implementation in current dynamic systems analysis and design software is presented. Example results based upon the analysis of a tracking task using three basic dynamic systems are compared with measured results and with similar analyses performed with the OCM and two previously proposed simplified optimal pilot models. The pilot frequency responses and error statistics obtained with this modified optimal control model are shown to compare more favorably to the measured experimental results than the other previously proposed simplified models evaluated.

14. SUBJECT TERMS
Manual vehicular control; Pilot modelling; Flying qualities

15. NUMBER OF PAGES
27

16. PRICE CODE
A03

17. SECURITY CLASSIFICATION OF REPORT Unclassified	18. SECURITY CLASSIFICATION OF THIS PAGE Unclassified	19. SECURITY CLASSIFICATION OF ABSTRACT	20. LIMITATION OF ABSTRACT